

## Supporting Information

### **Coordinated Sub-cycle Modulation Atomic Layer Deposition of Atomic-level Homogeneous GeTe<sub>2</sub> Thin Film for High-performance OTS**

Yunfei Hu,<sup>‡a</sup> Rongjiang Zhu,<sup>‡a</sup> Lun Wang,<sup>a</sup> Ke Gao,<sup>a</sup> Jinyu Wen,<sup>b</sup> Hao Tong<sup>ac\*</sup> and  
Xiangshui Miao<sup>ac</sup>

<sup>a</sup>School of Integrated Circuits, Huazhong University of Science and Technology,  
Wuhan 430074, China

<sup>b</sup>School of Artificial Intelligence and Automation, Huazhong University of Science and  
Technology, Wuhan 430074, China

<sup>c</sup>Hubei Yangtze Memory Laboratories, Wuhan 430205, China

[\\*tonghao@hust.edu.cn](mailto:tonghao@hust.edu.cn)

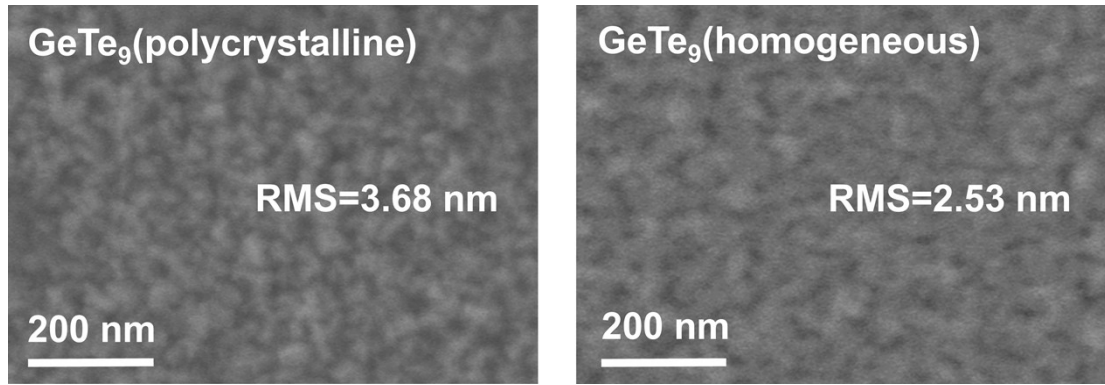


**Figure S1.** SEM images of GeTe<sub>9</sub> (polycrystalline) and GeTe<sub>9</sub> (homogeneous).

Figure S1 compares the surface morphology of GeTe<sub>9</sub> films synthesized under different sub-cycle conditions. The polycrystalline GeTe<sub>9</sub> film exhibits a relatively rough surface with a RMS roughness of 3.68 nm, which is attributed to the irregular grain growth and high grain-boundary density caused by insufficient precursor flux. In contrast, the homogeneous GeTe<sub>9</sub> film produced via the CSM strategy demonstrates a significantly smoother and more uniform surface with a reduced RMS roughness of 2.53 nm. This improvement confirms that the precise regulation of the super-cycle thickness to match the atomic diffusion length effectively suppresses the formation of large crystalline clusters, resulting in a more integrated and isotropic amorphous matrix.

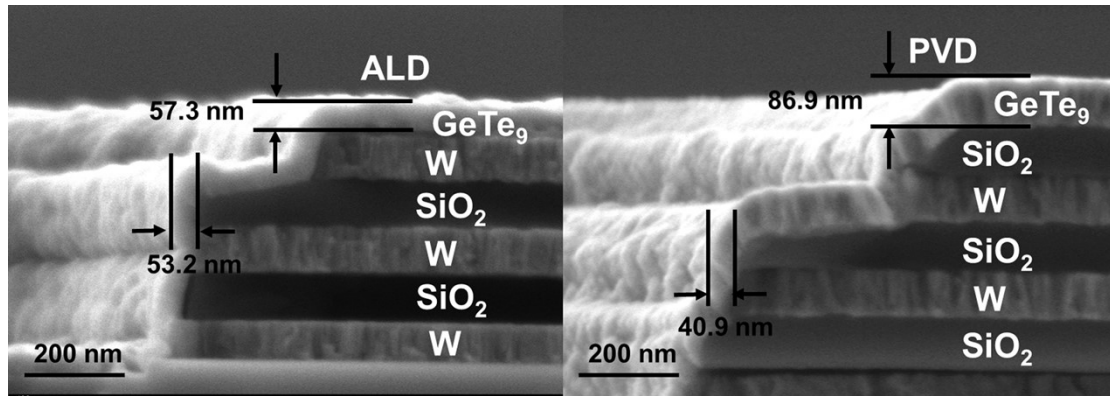


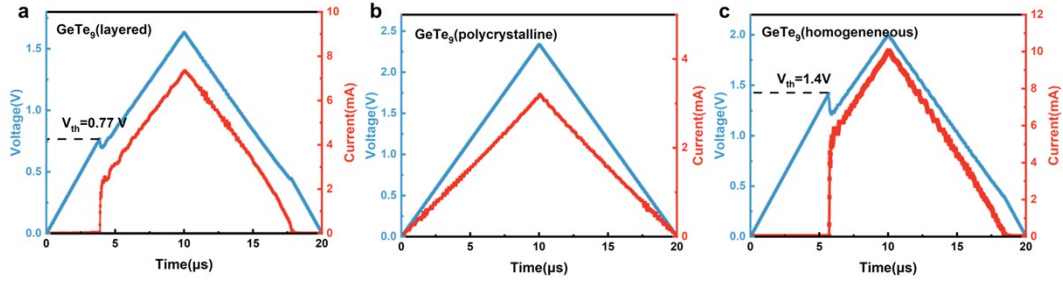
**Figure S2.** Comparison of step coverage between ALD and PVD deposited films.

The cross-sectional SEM images in Figure S2 illustrate the deposition of the  $\text{GeTe}_9$  film onto a 3D stacked structure for vertical integration composed of W and  $\text{SiO}_2$  layers. This comparison highlights the irreplaceable advantage of ALD over PVD for such complex high-aspect-ratio features. The ALD-deposited film exhibits excellent conformal growth across the W/ $\text{SiO}_2$  stack, maintaining a sidewall thickness of 53.2 nm relative to a top thickness of 57.3 nm, which corresponds to a step coverage of approximately 93%. Conversely, the PVD-deposited film shows poor conformality due to the inherent shadowing effect, where the sidewall thickness is significantly reduced to 40.9 nm compared to 86.9 nm at the top surface, yielding a step coverage of only 47%. These results validate that the ALD-CSM approach provides the high-precision conformal filling required for advanced 3D memory architectures.

**Table S1.** Comparison of film properties deposited by ALD (CSM strategy) and PVD.

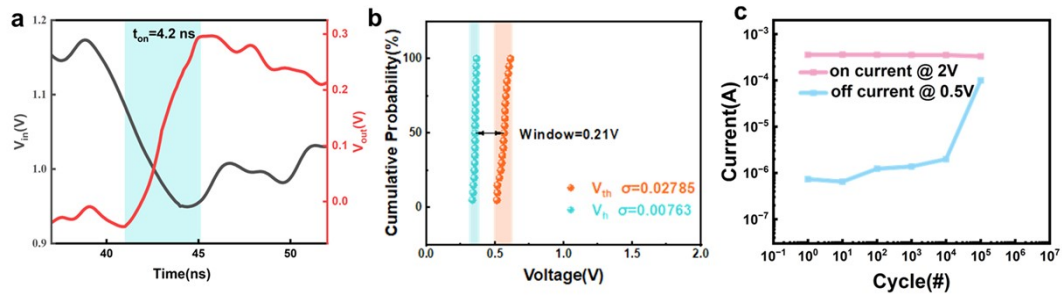
	ALD (This work, CSM)	PVD
Depositional state	Amorphous	Amorphous
Crystallization temperature	250 °C	131 °C <sup>[1]</sup>
RMS	2.53 nm	1.25 nm <sup>[2]</sup>
Step Coverage	93%	47%

Table S1 provides a quantitative benchmarking of GeTe<sub>9</sub> film properties synthesized by ALD and PVD. Both films remain in the amorphous state upon deposition. The amorphous structure of the ALD film is maintained up to 200 °C, providing an experimental reference for the thermal stability of Te-rich OTS selectors. While the PVD film exhibits lower surface roughness, its primary deficiency lies in the poor step coverage. In contrast, the ALD film synthesized via the CSM strategy achieves a superior step coverage of 93%, which is nearly double that of the PVD counterpart (47%), demonstrating its significant advantage for 3D vertical integration.



**Figure S3.** Triangular wave response of the three devices.

Figure S3 illustrates the transient switching characteristics of the three types of GeTe<sub>9</sub> devices under triangular voltage sweeps. The GeTe<sub>9</sub> (layered) device (a) exhibits a relatively low threshold voltage of approximately 0.77 V due to the presence of Te-rich pathways. The GeTe<sub>9</sub> (polycrystalline) device (b) fails to show any threshold switching behavior and instead presents a purely resistive response, indicating structural degradation and uncontrolled leakage. In stark contrast, the homogeneous GeTe<sub>9</sub> device (c) demonstrates an ideal OTS response with a high and stable threshold voltage of 1.4 V and excellent reversibility. This comparison corroborates that achieving atomic-level homogeneity is the fundamental prerequisite for reliable and high-performance switching operation.



**Figure S4.** Electrical characteristics of GeTe<sub>9</sub> (layered). (a) Switching speed of GeTe<sub>9</sub> (layered). (b) Threshold stability of GeTe<sub>9</sub> (layered). (c) Cycle endurance of GeTe<sub>9</sub> (layered).

The electrical performance of the GeTe<sub>9</sub> (layered) device is presented in Figure S4 for comparative analysis. As shown in Figure S4(a), the device achieves a switching speed of 4.2 ns. Figure S4(b) illustrates the  $V_{th}$  characteristics, where the GeTe<sub>9</sub> (layered) device exhibits a low  $V_{th}$  and a notably narrow switching window of 0.21 V. This specific dataset was recorded for only 40 cycles because the layered device is highly prone to functional failure during testing. This inherent instability is further evidenced in Figure S4(c), where the cycle endurance is limited to only  $10^4$  cycles, representing a significant five-order-of-magnitude decrease compared to the  $10^9$  cycles achieved by the CSM-optimized GeTe<sub>9</sub> (homogeneous) device.

#### Reference:

- [1] L. Wang, J. Wen, Z. Liu, J. Chen, H. Tong and X. Miao, Thermally stable and high-speed Ge-Te based ovonic threshold switching selector with a Ge intercalated structure, *IEEE Electron Device Lett.*, 2023, **44**, 1096–1099.
- [2] A. Manivannan, S. K. Myana, K. Miriyala, S. Sahu and R. Ramadurai, Low power ovonic threshold switching characteristics of thin GeTe<sub>6</sub> films using conductive atomic force microscopy, *Appl. Phys. Lett.*, 2014, **105**, 243501.